行政院國家科學委員會專題研究計畫　成果報告

結合磁共振造影與計算流力技術之人體主動脈的數值模擬

(II)

計畫類別：個別型計畫
計畫編號：NSC94-2213-E-216-025-
執行期間：94 年 08 月 01 日至 95 年 07 月 31 日
執行單位：中華大學機械工程學系

計畫主持人：牛仰堯

計畫參與人員：Chin-Hung Chang and Wen-Yih I. Tseng, Hsu-Hsia Peng

報告類型：精簡報告
報告附件：出席國際會議研究心得報告及發表論文
處理方式：本計畫涉及專利或其他智慧財產權，2 年後可公開查詢

中　華　民　國 95 年 10 月 26 日

Simulation of Blood Flows through a Dynamic Aorta

Yang-Yao Niu , Chin-Hung Chang[1] and Wen-Yih I. Tseng[2] Hsu-Hsia Peng[3]

1. Institute of Mechanical Engineering, Chung Hua University Hsin Chu, Taiwan 300, ROC

2. National Taiwan University Hospital Taipei, ROC

3. Department of Electrical Engineering, National Taiwan University, Taipei, ROC

1. Abstract

Blood flows and vessel wall shear stress distributions in a human aortic arch have been predicted numerically for a Reynolds number of 5000 at entrance. The simulated geometry was derived from the three-dimensional reconstruction of a series of two-dimensional slices obtained in vivo. Numerical results demonstrate wall shear stresses were highly dynamic, but were generally high along the outer wall in the vicinity of the branches and low along the inner wall, particularly in the descending thoracic aorta. The maximum wall stress distribution is presented on the aortic arch in the systole. Extensive secondary flow motion was observed in the aorta, and the structure of these secondary flows was influenced considerably by the presence of the branches. Within the aorta, both numerical results and MRI data observed that clockwise secondary flow recirculation appears in the upstream of aortic arch in the late systolic and turn out to be a pair of counter-clockwise vortex in the downstream of the arch in the early diastole. In addition, it is also observed the secondary flow in middle and right branches and violent rotation in left branch.

Keywords; Aorta, Newtonian Flows, Secondary Flow, Wall shear Stress

2. Introduction

In recent years, National Health Administration of Taiwan has announced that cerebrovascular and cardiovascular diseases had already become the major causes of the death. The cardiovascular diseases mainly include atherosclerotic, aortic dissection, artery stenosis and aortic aneurysm. The past researches [1-2] have shown the homodynamic such as blood circulation, vessel wall pressure and shear stress distributes and morphology of the vessel (like bifurcation branch, aorta arch and irregular tube) may play important roles in the formation of the cardiovascular diseases. Clinical observations also show that the region near the aortic arch is one of the sites where the cardiovascular diseases develop frequently. In this region, blood circulation will produce flow separation, secondary flow, three-dimensional vortex which cause very complicated hemodynamics. In those researches, there are always shown that the distribution of shear stress on the vessel wall was regarded as the main factor to influence arterial deformity. The maximum of the wall stress was shown to occur at the area which the vortex and secondary flow appears. Therefore, the understanding of the blood flow motion in the arterial vessel is highly required and will be the main goal in our simulation.

In the work, a numerical test model was derived from the three-dimensional reconstruction of a series of two-dimensional slices obtained in vivo using Magnetic Resonance Imaging(MRI) provided by National Taiwan University hospital on a human aorta. The inlet and out let aortic boundary conditions were also obtained by the image files from the MRI. Those image data include velocity vector distribution in cross section A, B, C, D as shown in Figure 1 and 2. Aorta, Brachiocephalic artery (BA), Left common carotid artery (CA), Left subclavian artery (SA), and its velocity and flow rate composed of three direction(u, v, w) are shown in Figure 3. Blood flows and vessel wall shear stress distributions in a human aortic arch will be simulated.

3. Numerical Model

In this study, we generate the geometry for this study, a series of aortic slices of a human aorta (A healthy young man) were acquired in vivo using MRI. The MRI data consisted of many curves of main aortic and three bifurcations cross-section. Because the MRI data of aorta have too many curves that can't construct the model easily, we simplify curves and reconstruct the geometry in CFX5 flow package. Coordinate data for the centerline was extracted for the aorta and three branches from the 3-D reconstructed MR image. Those data were curve-fitted to the cubic spline function, and the cross sectional grids were generated on the normal planes defined by the principal normal and binormal, at discrete equidistant points along the centerline curve. Using

this cross section definition, a computable model can be constructed because adjacent cross sections never overlap if the tube radius is smaller than that of curvature at the local point. The diameter of the tube was assumed to be uniform. The diameters of AA, BA, CA, and SA were 2 cm, 1 cm, 0.7 cm, and 0.7 cm, respectively. The model is shown in Fig. 1. The three branches were overlapped with the aortic arch model at the parts of those inlet sections as shown in Fig. 1 using a chimera meshing technique. A commercial CFD program, CFX version 5.5 was used for the computations. The following 3-D unsteady Navier-Stokes equations were solved: boundaries: (1) the inlet of the arch model, (2) the outlet of each model, (3) the wall regions which do not overlap with other model, and (4) the overlapped regions which are embedded in other model.

The following conditions for these boundaries were used:

(1) A MRI scan inflow rate at the inlet.

(2) Zero pressure and zero velocity gradients at the outlet of aorta.

(3) No-slip at the wall regions.

(4) MRI scan outflow rate are assumed at the outlet of three branches. The properties of water were used for the working fluid. The Reynolds number defined using the diameter, and the inflow velocity was 5000. Also, the three-dimensional, time-dependent, incompressible Navier-Stokes equations are solved by means of a commercial CFX5 package. It adopts a SIMPLE type finite volume method with a third-order accurate QUICK differencing scheme for all equations. The flow was assumed to be incompressible and Newtonian with turbulence assumption and the walls were rigid with no slip conditions.

4. Results and Discussions

In this part, an unstructured mesh approach is used together with body fitted meshes to model the flow in the aorta arch, and the following four separate computational meshes have been employed: one for the region spanning the ascending aorta along with the aortic arch and a portion of the descending aorta, and one of each of the three branches-the BA, CA and SA. The unstructured mesh allows for each section of the geometry to be meshed independently, and the individual meshes are subsequently coupled together by CFX-BUILD. We also assume the mesh is stationary in this case, and total grid numbers are 668764. The flow model is supposed be incompressible flow, unsteady flow and Newtonian flow, and we calculated the flow field in the aortic arch model with physiologically relevant Reynold's number of Re=5000. According MRI data, one cycle of heartbeat is 0.855 seconds, so we set a cycle as same as MRI data in numerical simulation. The calculations were performed a finite-volume formulation of the Navier-Stokes equations by the CFX5 Flow packages based on unstructured grids. The velocity field was found to satisfy the convergence criterion after starting the computation with zero velocity.

Figure 5 present the wall shear stress distributed. It is demonstrated that wall shear stresses were highly dynamic, but were generally high along the outer wall in the vicinity of the branches and low along the inner wall, particularly in the descending thoracic aorta. The maximum wall shear stress distribution is presented on the aortic arch in the late systole. According to previous researches, the position which has more changes of wall shear stress were occur the vessel pathological changes.

Figure 6 shows stream line distributed. We can clearly observe the blood flow through aorta and inner fluid field of aorta. When t = 2/6 T, we can find the vortex appears in the CA and SA, and it disappears after t = 3/6 T. We also can find the violent rotation in BA during 3/6 T and 4/6 T. Because flow rate is very lower in the late diastole, fluid field of blood does not have obvious change.

Figure 7 show the velocity vectors on the cross sections of the aorta at different time period. Extensive secondary flow motion was observed in the cross section D,F,G,H in the t = 3/6 T , and the structure of these secondary flows was influenced considerably by the presence of the branches. Also, it is observed that clockwise secondary flow recirculation appears in the downstream of aortic arch in the late systolic and turn out to be a pair of counter-clockwise vortex appearing in the turning corner of the aortic arch in the early diastole. However, the counter-clockwise vortex disappears in the upstream of the aorta arch and moves to the downstream of the descending aorta in the late diastole. These findings are largely consistent with previous experimental measurements in a model human aortic arch in which secondary flow structures coincides with as same as measurement of P. J. Kilner, et al.[1].

Also the cross section velocity vectors in the ascending aorta measured from MRA are shown in Figures 2. We can see the formation of a clockwise vortex is appearing in the late systole and in the whole diastole. The oberservations on the vortex in the ascending aorta is similar to the numerically predicted results in Figure 7 in which the clockwise

vortex at ascending part A-C only exists in the diastole. However, due to the smaller diameters of three branches and the descending aorta; the resolution of the MRA scan data was not as fine as the main aortic arch. Therefore, the cross section velocity vectors in these parts are not shown for the comparison.

5. Concluded Remarks

We reconstruct aorta model and boundary condition based on MRI in this study. Also our simulations found that

1. Wall shear stresses were highly dynamic, but were generally high along the outer wall in the vicinity of the branches and low along the inner wall. The maximum wall shear stress distribution is presented on the aortic arch in the early systole.
2. Minor three-dimensional secondary flows appear in middle and right branches and flow separation in right branch in the late systole.
3. Extensive secondary flow motion and three dimensional helical vortex motions were shown in the diastolic cycle.

6. Acknowledgements

The authors wish to acknowledge the NSC grants under NSC 94-2213-E-216 -025, also the supports of the computing facility of National Center for the High-Performance Computing, Taiwan, ROC.

7. References

[1]P. J. Kilner, Z. Y. Yang, R. H. Mohiaddin, D. N. Firmin and D. B. Longmore. (1993) Helical and retrograde secondary flow patterns in the aortic arch studied by three-dimensional magnetic resonance velocity mapping, Circulation, 88, pp 2235-2247.

[2]N. Shahcheraghi, H. A. Dwyer, A. Y. Cheer, A. I. Barakat and T. Rutaganira (2002) Unsteady and tree-dimensional simulation of blood flow in the human aortic arch, *Journal of Biomechanical Engineering*, Vol. 124, pp 378-387.

[3]Y. Y. Niu, P. C. Wu, H. Y. Yu, W. Y. Tseng and H. H. Peng (2004) Simulation of Vessel Wall Stress Distributions and Secondary Flows for Blood flow through a Normal Aorta with Three Branches, *Proc. The 11th National Computational Fluid Dynamics Conference,* Tai-Tung, Vol. 1, 1811, pp CFD-1811.

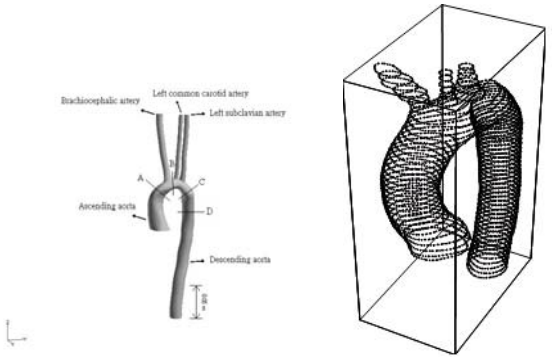

Figure 1. Schematic diagram of a normal aorta with a branch (Left), aorta outline scan by MRI (Right)

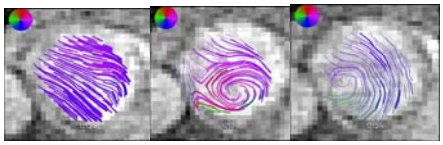

(A)

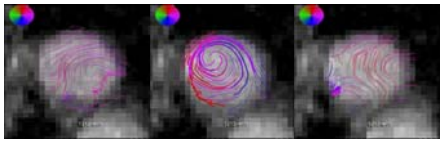

(B)

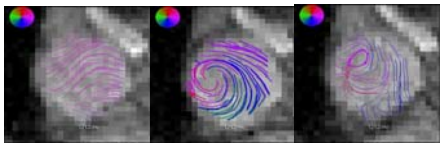

(C)

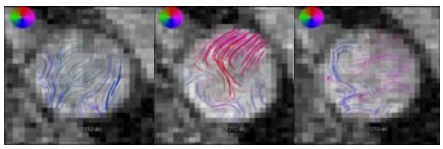

(D)

Figure 2. Velocity vector images at location A, B, C, D and at different time , scan by MRI

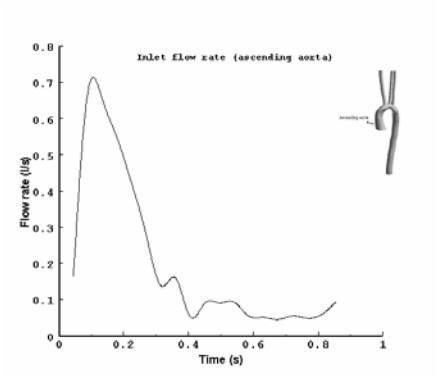

Figure 3. An entrance blood flow rate of Aorta measured from MRI

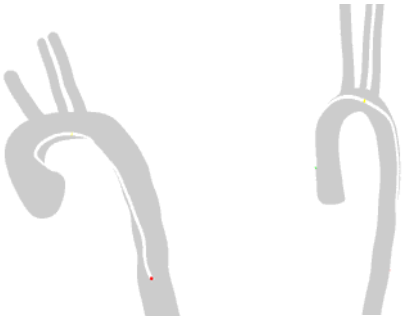

Figure 4. A diagram of inner and outer wall along Aortic Arch

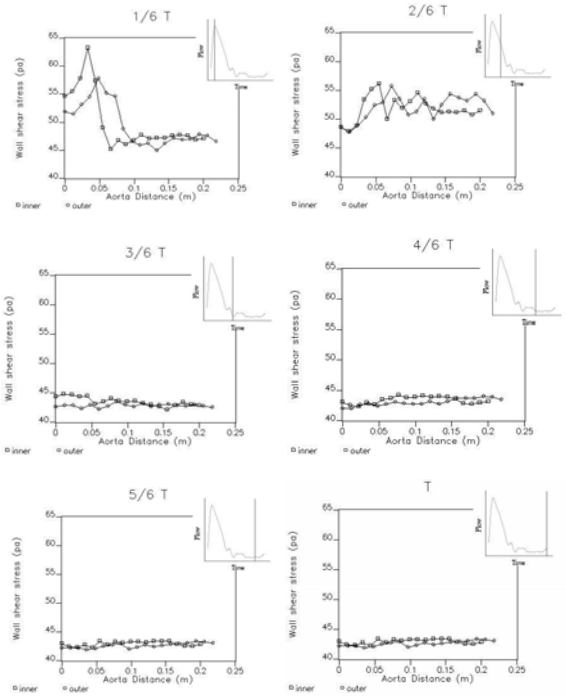

Figure 5. Wall shear stress distributions in a pulsatile cycle
(□—outer wall ○—inner wall)

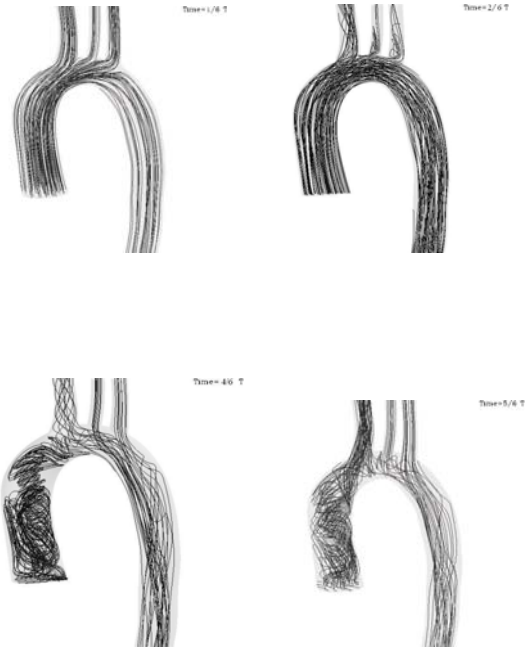

Figure 6. Stream line in aorta arch in a pusatile cycle

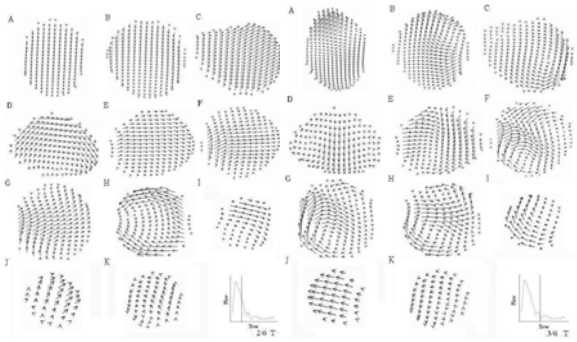

Figure 7. Velocity vectors on cross sections in a pusatile cycle

PCFD 2006 International Conference 學術研討會心得報告

中華大學機械系
報告人：牛仰堯

參加國際性會議不僅可以了解國外在相關領域的最新研究發展狀況， 同時也是與國外學者專家技術交流最直接最具經濟效益的方法之一。 因為一個成功的研討會，可以在短短的幾天中，聚集了來自各地達數百，甚至數千位學者專家於同一地點，做面對面直接的討論與溝通。 因此為求得在最短時間內獲取最新的資訊，參加謹慎選擇的國際性研討會，是最值得的。 本次會議 PCFD 2006 International Conference 於 5 月 15 日至 5 月 18 日舉行為 1 年一度的且有十餘年歷史之流體力學平行計算研討會，有來自各地的相關專家與學者，包括大學教授、研究人員、各國家實驗室的專職人員、工業界相關研究人員出席或發表論文。在會場上並有出版商提供各種流體力學平行計算相關專業書刊與資料，以及最新 Flow 電腦模擬所需的軟體所需的各項器材之展覽。

本次會議的地點在 Busan, Korea 會議於 5 月 14 日開始辦理報到註冊，主辦單位同時展示一些會議相關論文集及專業書刊，並有部份工作人員舉行會議前之準備集會。接下來的四天為正式的會議，包括專題演講、8 個邀請演講、專題討論及論文發表等議程。由大會依專業細分為 16 大項，論文發表以 2 個場地同時進行，共計有 16 場，每場約有 5-6 篇論文，會場外的大廳有軟體廠商、出版商與實驗器材廠商的展示及研究生之論文成果展。大會的子題包括了： Terascale computing, Mechanical and Aerospace Engineering,Industrial and Environmental Engineering, Medical and Biological Applications Atmospheric and Ocean Modeling, Combustion, Turbulence, Acoustics, Plasma Dynamics, Lattice Boltzmann Methods, Design Optimization Grid/Network Computing, Parallel Algorithms, Multi-scale and Multi-physics, Adaptive Mesh Refinement, Parallel Compiler and Software Development, Software Frameworks, Visualizatio. 由於場次眾多，個人僅能選擇性的參與 bio-fluid flows 論文發表。大本次會議台灣除筆者外，另外有清華、交通、大學教授學生近五人參與論文發表可謂盛況空前。

. 由本次研討會所發表的 100 餘篇論文及張貼海報可以看出，parallel CFD 領域本世紀發展之重要方向。。本次會議除了論文發表外，更有許多來自世界各地從事此一領域的學者專家齊聚一堂交換研究心得，探討各種 parallel computing 問題，不僅使參加者有機會發表自己的研究心得，更可了解他人的研究現況。藉著論文資料的蒐集，未來尚可提供國內相關研究人員會議狀況，對於促進國內 parallel CFD 科技研究，提升學術水準有莫大的助益。

Numerical Simulation of A Realistic Aortic Flow with MRA on Parallel Computers

Yang-Yao Niu[1] , Chin-Hung Chang[1,] Wen-Yih I. Tseng[2] Hsu-Hsia Peng[2] and Shou-Cheng Tcheng[3]

1. Institute of Mechanical Engineering, Chung Hua University Hsin Chu, Taiwan , ROC
2. National Taiwan University Hospital Taipei , ROC
3., The National Center for High-Performance Computing, Hsinchu, Taiwan ROC:
yniu@chu.edu.tw

Abstract A prototype, multi-scale, computational hemodynamic model is developed to predict blood flow patterns and wall stresses in a realistic human aorta. The three-dimensional model is utilized for blood flow simulation, which is based on Roe and HLLC type incompressible full Navier-Stokes equations and one-dimensional systematic arteries network models will be embedded into the future work. In this study, two- and three-dimensional secondary flows and vessel wall shear stress distributions in a human aortic arch have been predicted numerically for a Reynolds number of 5000 at entrance based on the techniques of CFD and MRA. The simulated geometry was derived from the three-dimensional reconstruction of a series of two-dimensional slices and several flow rates at different cross sections of aorta with the tree branches obtained from MRI. Numerical results demonstrate wall shear stresses were high along the outer wall in the vicinity of the branches and low along the inner wall, particularly in the descending thoracic aorta. The maximum wall stress distribution is presented on the aortic arch in the systole. Extensive secondary flow motion was observed in the aorta, and the structure of these secondary flows was influenced considerably by the presence of the branches. Within the aorta, both numerical results and MRI data observed that clockwise secondary flow recirculation appears in the upstream of aortic arch in the late systolic and turn out to be a pair of counter-clockwise vortex in the downstream of the arch in the early diastole. In addition, three-dimensional particle trace plots observe the secondary flows in middle and right branches and violent rotation in left branch.The original FORTRAN code is converted to the MPI code and tested on 32-CPU IBM SP2 Power 3 and Power 4 parallel computers and two 32-node PC Clusters.

Keywords; Aortic Flow Model, Riemann Solvers, Blood flow, MRI

Acknowledgements

The authors wish to acknowledge the NSC grants under NSC 94-2213-E-216-025, also the supports of the computing facility of National Center for the High-Performance Computing, Taiwan, ROC.

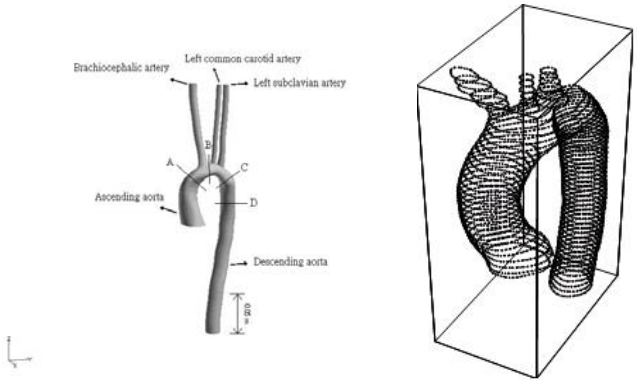

Figure 1 Schematic diagram of a normal aorta with a branch (Left), aorta outline scan by MRA (Right)

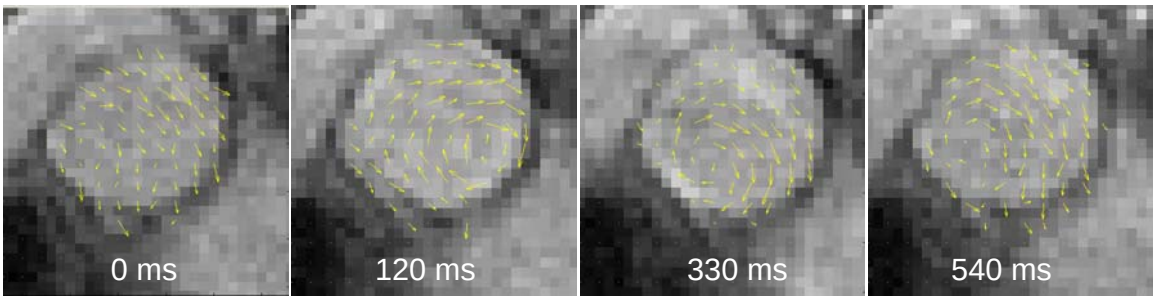

Figure 2 Velocity vector images scan by MRI

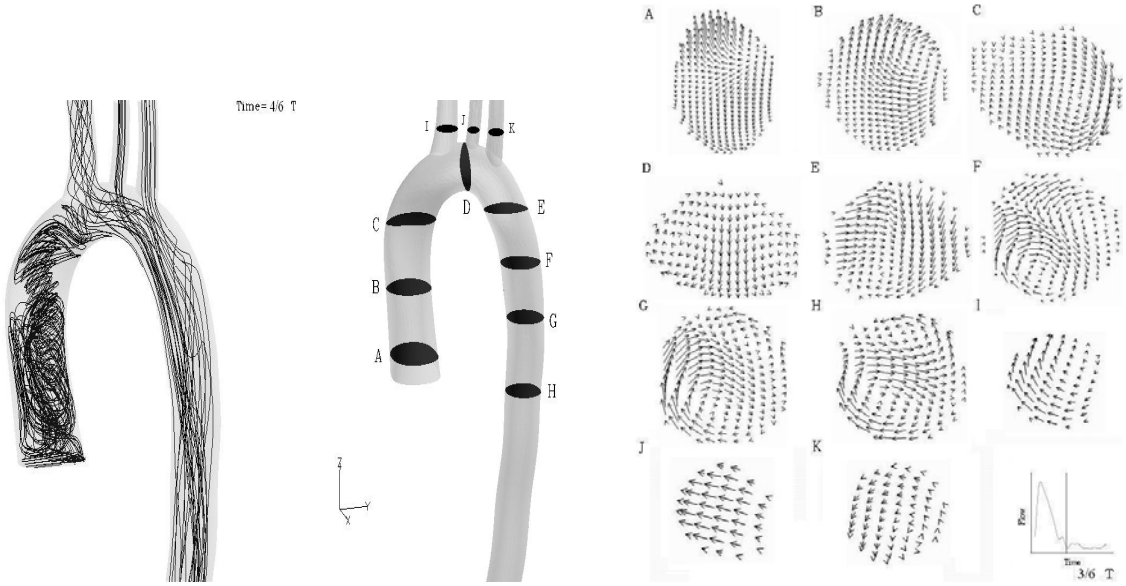

Figure 3 Particle traces in aorta and velocity vectors on cross sections in a diastolic cycle